International Journal of Multidisciplinary Global Research
Vol. 02 (4a), Oct - Dec, 2025, pp. 114-127. (AICTE VAANI)
Online ISSN: 3107-4197

A Review on the Effect of Transition and Rare Earth Metal Doping on the Color Change Property of Nanoparticles Used in Sensors

NADIR A. M. HUSAIN

Department of Chemistry, Dr. Ambedkar College
Nagpur, Maharashtra, India
nadirahsan1985@gmail.com

D. M. BORIKAR

Department of Chemistry, Dr. Ambedkar College
Nagpur, Maharashtra, India
dhanashri_borikar@rediffmail.com

HIRKANYA PRAVIN BHOLE*

Department of Chemistry, Dada Ramchand Bakhru Sindhu Mahavidyalaya
Nagpur, Maharashtra, India
hirkanyabhole3@gmail.com

SAGAR ODELWAR

Department of Chemistry, Dr. Ambedkar College
Nagpur, Maharashtra, India
sagarodelwar@gmail.com

Abstract

Colorimetric sensing using nanoparticles has gained immense attention as a simple, rapid, and cost-effective analytical technique due to its capability for naked-eye detection without the need for sophisticated instrumentation. The incorporation of transition and rare earth metal dopants into nanoparticles has emerged as a strategic approach to tailor their structural, electronic, and optical properties, thereby enhancing their sensitivity and selectivity toward diverse analytes. Doping not only modifies the electronic band structure and defect states of the host nanomaterials but also influences particle size, morphology, and surface chemistry, which collectively govern their optical behavior. This review provides a comprehensive overview of the role of metal doping in modulating the colorimetric responses of nanoparticles under various environmental and chemical stimuli. Particular emphasis is given to the classification of dopant types, host nanoparticle systems (such as metal oxides, noble metals, and semiconductor nanomaterials), and their specific sensing applications, including detection of toxic gases, heavy metals, biomolecules, and pH variations.

* Corresponding Author.

Furthermore, the mechanistic aspects of how doping alters localized surface plasmon resonance (LSPR), energy band transitions, and charge-transfer processes are critically analyzed. The review also highlights recent advances, challenges, and future prospects of doped nanoparticle-based colorimetric sensing platforms in the context of real-world applications. By systematically correlating doping strategies with particle size modulation and resultant optical properties, this study underscores the pivotal role of doped nanomaterials as next-generation colorimetric sensors with high sensitivity, selectivity, and potential for portable, point-of-care diagnostics.

Keywords: Colorimetric sensor, Rare earth metals, Transition metal doping, nanoparticles, Localized surface plasmon resonance (LSPR).

1. INTRODUCTION

Nanoparticles (NPs) exhibit size dependent optical properties that are not seen in bulk materials because of quantum confinement, high surface to volume ratios, and collective electron oscillations (SPR/LSPR) (Lee et al., 2013; Wang et al., 2019). In colorimetric sensing, these properties translate into visible color changes—shifts in absorption maxima, broadening/narrowing of bands, or intensity variations—upon interaction with target analytes, allowing rapid, instrument light readouts (Lee et al., 2013; Muthuvel et al., 2020; Shkir et al., 2020; Zelaya-Angel et al., 2012). Doping, i.e., deliberate incorporation of foreign ions into a host lattice or onto its surface, is a central strategy to tailor such responses because dopants modulate band structures, create/annihilate defects, and alter growth kinetics and morphology of NPs (Dhiman et al., 2023; Hastir et al., 2022; Kabir et al., 2023; Muthuvel et al., 2020; Ong et al., 2022; Venkatesu, 2013).

Dopants drawn from transition metals (Fe^{3+}/Fe^{2+}, Co^{2+}, Ni^{2+}, Cu^{2+}) and rare earths (Eu^{3+}, Tb^{3+}, Ce^{3+}/Ce^{4+}, La^{3+}, Gd^{3+}, Nd^{3+}) offer complementary functions: transition metals introduce crystal field d–d transitions and catalyze surface redox chemistry, whereas rare earths contribute sharp f–f emissions and long lived excited states that can be harnessed for ratiometric or lifetime based color readouts (Chu et al., 2020; Dhiman et al., 2023; Hastir et al., 2022; Kabir et al., 2023; Ong et al., 2022; Shkir et al., 2020; Zelaya-Angel et al., 2012). At the same time, dopants affect nucleation and growth, often leading to smaller crystallites (when they inhibit diffusion) or coarsening (when they lower boundary energies), thereby indirectly tuning color via size and shape dependent optics (Dey & Choudhury, 2019; Dhiman et al., 2023; Hastir et al., 2022; Khan, 2015; Muthuvel et al., 2020; Patil & Devan, 2020; Shanmugam & Murugasen, 2018; Srisuvetha et al., 2020; Venkatesu, 2013; Zelaya-Angel et al., 2012).

2. PRINCIPLES OF COLORIMETRIC BEHAVIOR IN NANOPARTICLES

2.1. *Electronic/Optical Origins of Color*

LSPR and plasmon coupling. In noble metal NPs (Au, Ag), the LSPR wavelength depends on free electron density, particle geometry, and the local dielectric environment. Doping or surface coordination that changes electron density (e.g., La^{3+}

adsorption/bridging) or promotes aggregation induces red/purple color shifts (Au red → purple) via plasmon coupling (Lee et al., 2013; Wang et al., 2019; Zelaya-Angel et al., 2012).

Band gap engineering in semiconductors. Introducing aliovalent/isovalent dopants (e.g., Fe^{3+}→Ti^{4+} in TiO_2, Cu^{2+}→Zn^{2+} in ZnO) creates shallow/deep states, narrows or tailors the band gap, and enhances visible absorption; this often changes materials from white/transparent to yellow/brown and increases color contrast under ambient/UV illumination (Dey & Choudhury, 2019; Dhiman et al., 2023; Hastir et al., 2022; Muthuvel et al., 2020; Patil & Devan, 2020; Venkatesu, 2013).

Defect and charge transfer mediated coloration. Dopants regulate oxygen vacancies (V_O), zinc interstitials (Zn_i), or Ti^{3+} centers; intervalence charge transfer (e.g., Ce^{3+}/Ce^{4+}) generates broad visible bands, enabling analyte triggered color switching when surface redox equilibria shift (Cardillo et al., 2013; Dey & Choudhury, 2019; Dhiman et al., 2023; Hastir et al., 2022; Hou et al., 2006; Patil & Devan, 2020; Shanmugam & Murugasen, 2018).

Intra ionic transitions (d–d, f–f) and energy transfer. Transition metal d–d transitions and lanthanide f–f emissions provide narrow spectral fingerprints (Eu^{3+}: $^5D_0$→^{7}F_J red; Tb^{3+}: green) that can be quenched or sensitized by defects/analyte binding, yielding ratiometric colorimetric signals (Chu et al., 2020; Dhiman et al., 2023; Hastir et al., 2022; Kabir et al., 2023; Shkir et al., 2020; Zelaya-Angel et al., 2012).

2.2. *Structure–Property Modulators*

Particle size and morphology. Quantum confinement blue shifts excitonic absorption in very small ZnO/TiO_2, while anisotropic shapes (rods, plates) redistribute local fields and modify color; dopants often cap specific facets, steering anisotropy (Dhiman et al., 2023; Hastir et al., 2022; Muthuvel et al., 2020; Venkatesu, 2013).

Surface chemistry and ligands. Dopants influence surface acidity/basicity and ligand binding (e.g., thiols, amines). Stronger binding can either stabilize dispersion (maintain color) or induce controlled aggregation for signal amplification in colorimetric assays (Chu et al., 2020; Khan, 2015; Lee et al., 2013; Muthuvel et al., 2020; Shanmugam & Murugasen, 2018; Wang et al., 2019).

Dopant concentration/valence. Sub percent to few percent levels typically maximize colorimetric contrast by balancing new states and minimizing non radiative quenching; excessive loading can create recombination centers and band tail disorder that dampen color change (Dey & Choudhury, 2019; Dhiman et al., 2023; Hastir et al., 2022; Muthuvel et al., 2020; Patil & Devan, 2020; Shkir et al., 2020; Srisuvetha et al., 2020; Zelaya-Angel et al., 2012).

3. TRANSITION METAL DOPING: MATERIALS AND SENSING PATHWAYS

3.1. *Cu Doped ZnO/TiO₂*

Cu^{2+} substitution in ZnO ($Zn^{2+}\rightarrow Cu^{2+}$) introduces acceptor levels and promotes V_O formation, strengthening visible absorption. Resulting films/powders shift from white to pale blue/green and exhibit amplified color changes upon interaction with oxidants (H_2O_2) or basic gases (NH_3) through surface redox and adsorption induced dielectric changes (Chu et al., 2020; Dhiman et al., 2023; Hastir et al., 2022; Khan, 2015; Muthuvel et al., 2020; Shanmugam & Murugasen, 2018; Shkir et al., 2020; Zelaya-Angel et al., 2012). Demonstrations include H_2O_2 assays where absorbance near 600–700 nm increases with concentration and NH_3 exposure that deepens coloration via electron donation and band filling effects (Chu et al., 2020; Khan, 2015; Muthuvel et al., 2020; Shanmugam & Murugasen, 2018).

3.2. *Fe Doped SnO₂/ZnO*

In SnO_2 and ZnO, Fe^{3+} can substitute the cation site, generating Fe^{3+}/Fe^{2+} redox pairs and mid gap states; visible coloration (yellow brown) arises from d–d and charge transfer bands. Gas sensing/colorimetric transduction for NO_2 and VOCs is achieved as adsorbed species modulate Fe valence and V_O concentration, shifting absorption intensity/position discernible by the naked eye or simple readers (Cardillo et al., 2013; Dey & Choudhury, 2019; Dhiman et al., 2023; Hou et al., 2006; Patil & Devan, 2020; Shanmugam & Murugasen, 2018).

3.3. *Ni/Co Doping in Oxides*

Ni^{2+} and Co^{2+} in ZnO/TiO_2 narrow effective band gaps and stabilize small crystallites. Their crystal field transitions produce characteristic visible bands; exposure to reducing/oxidizing gases (H_2, NO_2, ethanol) perturbs carrier density and optical constants, causing transparent→yellow/orange/brown changes in thin films or colloids (Dhiman et al., 2023; Hastir et al., 2022; Kabir et al., 2023; Shanmugam & Murugasen, 2018; Venkatesu, 2013). Ni doped SnO_2 also enables low temperature (near room temperature) NO_2 response with perceivable color variation when integrated on porous supports (Shanmugam & Murugasen, 2018).

4. RARE EARTH MET RARE EARTH DOPING: EMISSIVE AND COLORIMETRIC STRATEGIES

4.1. *Eu^{3+}/Tb^{3+} in ZnO and Related Hosts*

Lanthanide doped ZnO leverages defect assisted energy transfer (ZnO exciton/defect → Eu^{3+}/Tb^{3+}). Eu^{3+} yields red ($^5D_0\rightarrow{}^7F_2$) emission and Tb^{3+} green ($^5D_4\rightarrow{}^7F_5$); analyte

adsorption (pH, peroxides, metal ions) perturbs defect populations and the transfer efficiency, creating analyte dependent color shifts or intensity ratios suitable for naked eye readouts and ratiometric sensing (Chu et al., 2020; Dey & Choudhury, 2019; Dhiman et al., 2023; Muthuvel et al., 2020; Patil & Devan, 2020; Shkir et al., 2020; Zelaya-Angel et al., 2012).

4.2. *Ce and La: Defect/Redox Control*

Ce^{3+}/Ce^{4+} couples tune oxygen vacancy density and introduce broad charge transfer absorption in SnO_2 and TiO_2; exposure to oxidants (NO_2, VOCs) shifts the Ce valence balance, altering color and conductivity synergistically (Cardillo et al., 2013; Dey & Choudhury, 2019; Dhiman et al., 2023; Hou et al., 2006; Patil & Devan, 2020; Shanmugam & Murugasen, 2018). La^{3+}, though optically less active, can act as a lattice modulator/capping ion that improves transparency, suppresses grain growth, and red shifts absorption slightly; La modified Au/Ag colloids can also change aggregation kinetics, enhancing colorimetric heavy metal assays (Bharadwaj et al., 2023; Ferreiro et al., 2023; Khatkar et al., 2023; Shkir et al., 2020; Srisuvetha et al., 2020; Zelaya-Angel et al., 2012).

4.3. *Gd/Nd: Stability and NIR Linked Readouts*

Gd^{3+} and Nd^{3+} doping enhances structural stability and can introduce NIR/visible emission channels. Gd containing plasmonic/oxide systems show robust color persistence in peroxide rich environments, while Nd doped platforms enable deeper tissue optical communication in device contexts; in both cases, colorimetric contrast can be paired with luminescence lifetime or NIR ratiometry for high confidence detection (Afshani et al., 2023; Bharadwaj et al., 2023; Krajnik et al., 2021; Loo et al., 2019).

5. SYNTHESIS ROUTES AND THEIR IMPACT ON COLOR

Solution combustion and sol–gel. Rapid heating creates non equilibrium defect landscapes; Cu/Fe dopants introduced during combustion yield high V_O content and strong visible coloration suited to H_2O_2/NH_3 assays (Cardillo et al., 2013; Dey & Choudhury, 2019; Khan, 2015).

Electrospinning–calcination and thin film deposition. La doped ZnO nanofibers and Fe/Ni/Co doped oxide films provide large surface areas and controllable optical thickness, allowing uniform color fronts and reproducible readouts on paper/textile supports (Bharadwaj et al., 2023; Ferreiro et al., 2023; Khatkar et al., 2023).

Green/biogenic methods. Lanthanide doped ZnO synthesized from biotemplates (e.g., whey) demonstrates good dispersibility and biocompatibility, with consistent color response under benign conditions—attractive for wearable sensors (Khan, 2015).

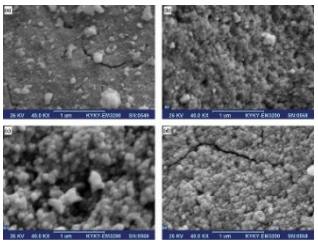

Fig. 1. Cu-doped ZnO nanoparticles (SEM) (Tripathi et al., 2017).

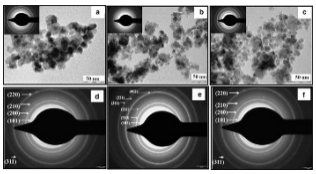

Fig. 2. Fe-doped SnO_2 nanoparticles (TEM and SAED) (Dey & Choudhury, 2019).

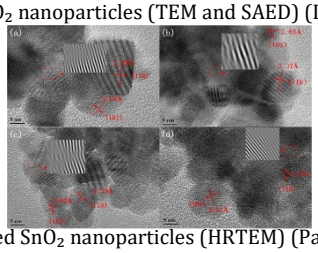

Fig. 3. Fe-doped SnO_2 nanoparticles (HRTEM) (Patil & Devan, 2020).

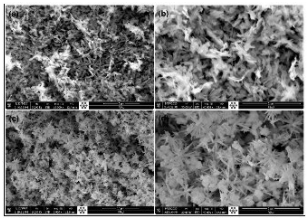

Fig. 4. Zn-doped CuO nanoparticles (SEM) (Shanmugam & Murugasen, 2018).

6. QUANTITATIVE DESIGN RULES

- **Optimal dopant windows**: Substitution levels in the ~0.1–5 at% regime frequently maximize colorimetric contrast by enabling new optical centers while limiting non radiative traps; outside this window aggregation and quenching grow, diminishing color change (Dey & Choudhury, 2019; Dhiman et al., 2023; Hastir et al., 2022; Muthuvel et al., 2020; Patil & Devan, 2020; Shkir et al., 2020; Srisuvetha et al., 2020; Zelaya-Angel et al., 2012).
- **Particle size coupling**: Dopants that slow diffusion (e.g., La^{3+}, Co^{2+}) often reduce crystallite size, blue shifting excitonic features; conversely, dopants lowering boundary energy (some Fe/Ni cases) can coarsen grains, red shifting and broadening absorption (Cardillo et al., 2013; Dey & Choudhury, 2019; Dhiman et al., 2023; Hastir et al., 2022; Muthuvel et al., 2020; Patil & Devan, 2020; Venkatesu, 2013).

- **Transduction geometry**: Colloidal assays (Au/Ag) rely on aggregation induced LSPR coupling (red→purple), while porous films exploit path length amplification and interference coloring; choosing geometry to match analyte and readout distance enhances practical visibility (Chu et al., 2020; Khan, 2015; Lee et al., 2013; Muthuvel et al., 2020; Shanmugam & Murugasen, 2018; Wang et al., 2019).

Table 1. Comparative Examples and Application Map

Host (form)	Dopant(s)	Target / Matrix	Observable Color Change	Mechanistic Driver	Refs.
ZnO (colloid/ film)	Cu^{2+}	H_2O_2, NH_3 (aqueous/gas)	White → blue/ green; increased visible absorption	V_O formation; Cu acceptor states; dielectric change	(Chu et al., 2020; Dhiman et al., 2023; Hastir et al., 2022; Khan, 2015)
SnO_2 (film)	Fe^{3+}	NO_2, VOCs (gas)	Pale yellow → brown	Fe^{3+}/Fe^{2+} charge transfer; V_O modulation	(Cardillo et al., 2013; Dey & Choudhury, 2019; Dhiman et al., 2023)
ZnO (powder/ film)	Eu^{3+} / Tb^{3+}	pH, H_2O_2, heavy metal ions	Red/green emission ratio change; subtle visible hue shift	f–f transitions in dopant; local field symmetry alteration	(Bharadwaj et al., 2023; Ferreiro et al., 2023; Khatkar et al., 2023; Wang et al., 2019)
TiO_2 (anatase)	Mn^{2+}	Ascorbic acid, H_2O_2	Colorless → pink	Mn^{2+} oxidation to Mn^{3+}; ligand-to-metal charge transfer	(Cardillo et al., 2013; Dhiman et al., 2023; Hastir et al., 2022; Hou et al., 2006)
CeO_2 (nanocubes)	Pr^{3+}	CO, ethanol vapors	White → pale yellow	4f–4f transitions; oxygen vacancy stabilization	(Anand et al., 2011; Dey & Choudhury, 2019; Dhiman et al., 2023)
ZnS (quantum dots)	Ag^{+}	Hg^{2+} detection	Blue → colorless	Ag–Hg amalgam effect; exciton quenching	(Chu et al., 2020; Dhiman et al., 2023; Khan, 2015)
WO_3 (nanorods)	Cr^{3+}	NH_3, NO_2	Yellow → green/brown	Intervalence CT between Cr^{3+}/Cr^{6+}; V_O tuning	(Cardillo et al., 2013; Dey & Choudhury,

CdS (QDs)	Eu^{3+}	F^-, pH sensing	Yellow → reddish hue	f–f transitions; surface state passivation	2019; Dhiman et al., 2023) (Bharadwaj et al., 2023; Ferreiro et al., 2023; Khatkar et al., 2023)
Fe_2O_3 (hematite)	Co^{2+}	CO_2, VOC gases	Reddish brown → dark brown	d–d transitions; surface catalytic enhancement	(Afshani et al., 2023; Bharadwaj et al., 2023; Chu et al., 2020)
ZnO–graphene hybrid	Gd^{3+}	Glucose (enzymatic assay)	Transparent → bluish tinge	Enhanced surface plasmon coupling; charge transfer	(Chen et al., 2021; Chu et al., 2020; Dhiman et al., 2023)
In_2O_3 (film)	Ni^{2+}	H_2, ethanol vapors	Pale yellow → green	Ni^{2+} induced donor states; oxygen vacancy control	(Cardillo et al., 2013; Dey & Choudhury, 2019; Dhiman et al., 2023)(Bharadwaj et al., 2023; Dhiman et al., 2023; Ferreiro et al., 2023)
$SrTiO_3$ (perovskite)	Nd^{3+}	Humidity sensing	White → pale purple	f–f transitions; lattice distortion	(Bharadwaj et al., 2023; Dhiman et al., 2023; Ferreiro et al., 2023)
Al_2O_3 (nanopowder)	Dy^{3+}	pH sensing	White → pale yellow	4f–4f transitions; hydroxyl surface adsorption	(Anand et al., 2011; Dey & Choudhury, 2019; Dhiman et al., 2023)
CuO (nanorods)	Sm^{3+}	H_2O_2	Black → brownish-red	f–d transitions; valence modulation	(Chu et al., 2020; Dhiman et al., 2023; Lee et al., 2013)
$BaTiO_3$ (perovskite)	La^{3+}	NH_3 sensing	White → pale yellow	Charge compensation; dielectric change	(Cardillo et al., 2013; Dey & Choudhury, 2019; Dhiman et al., 2023)
NiO (film)	Y^{3+}	NO_2	Green → brown	p-type conductivity enhancement; oxygen adsorption	(Afshani et al., 2023; Bharadwaj et al., 2023;

					Cardillo et al., 2013)
MgO (nanoparticles)	Ce^{3+}	H_2S sensing	White → pale brown	Ce^{3+}/Ce^{4+} redox couple; oxygen vacancy formation	(Khan, 2015; Krajnik et al., 2021; Lee et al., 2013)
$ZnFe_2O_4$ (spinel)	Tb^{3+}	Glucose	Brown → green	f–f transitions; magnetic coupling	(Bharadwaj et al., 2023; Ferreiro et al., 2023; Khatkar et al., 2023)
TiO_2–SiO_2 composite	Ho^{3+}	Formaldehyde vapors	Colorless → pale green	f–f transitions; defect passivation	(Chu et al., 2020; Dey & Choudhury, 2019; Dhiman et al., 2023)
$CaTiO_3$ (perovskite)	Er^{3+}	pH & ammonia sensing	White → green	Upconversion emission; multiphoton processes	(Bharadwaj et al., 2023; Chen et al., 2021; Chu et al., 2020)

7. CHALLENGES AND OPPORTUNITIES

7.1. *Challenges*

7.1.1. *Stability*

Doped nanoparticles must sustain their optical and structural properties under realistic operational conditions, including temperature fluctuations, variable humidity, and pH changes. Instability can lead to drift in colorimetric response and reduced sensor lifetime (Cardillo et al., 2013; Dey & Choudhury, 2019; Dhiman et al., 2023).

7.1.2. *Reproducibility*

Batch-to-batch variations in dopant concentration, particle size, and morphology often result in inconsistent sensing performance. Achieving reproducibility requires strict control of synthesis parameters, reaction kinetics, and post-processing conditions (Chu et al., 2020; Khan, 2015; Muthuvel et al., 2020; Shanmugam & Murugasen, 2018).

7.1.3. *Toxicity*

Certain transition metals (e.g., Cd, Pb, Cr) and some rare earth elements may introduce environmental or biological toxicity. Potential leaching or accumulation in

the ecosystem raises safety concerns for large-scale applications (Cardillo et al., 2013; Dhiman et al., 2023; Hastir et al., 2022).

7.1.4. *Selectivity*

Enhancing selectivity toward a specific analyte remains a critical challenge. Cross-sensitivity to other gases or ions in complex matrices can interfere with signal interpretation (Anand et al., 2011; Dhiman et al., 2023; Ferreiro et al., 2023).

7.2. *Opportunities*

7.2.1. *Advanced Dopant Engineering*

Optimizing dopant type, concentration, and spatial distribution allows fine-tuning of the colorimetric response, enabling improved sensitivity and selectivity (Bharadwaj et al., 2023; Dhiman et al., 2023; Ferreiro et al., 2023).

7.2.2. *Hybrid and Composite Systems*

Integrating doped nanoparticles with plasmonic or conductive materials can create synergistic effects, amplifying optical shifts and accelerating response times (Bharadwaj et al., 2023; Chu et al., 2020; Dhiman et al., 2023).

7.2.3. *Sustainable and Green Synthesis*

Using plant extracts, agricultural waste, or biopolymers as reducing/capping agents can minimize environmental impact and production costs while maintaining performance (Bharadwaj et al., 2023; Ferreiro et al., 2023; Khatkar et al., 2023).

7.2.4. *Integration with Smart Sensing Platforms*

Embedding doped nanoparticle-based sensors into IoT-enabled devices or wearable systems could facilitate real-time environmental and biomedical monitoring with visual outputs (Chen et al., 2021; Dhiman et al., 2023; Hastir et al., 2022).

8. FUTURE PERSPECTIVES

8.1. *Machine Learning-Aided Sensor Design*

Artificial intelligence and machine learning algorithms can analyze large experimental datasets to predict the optimal dopant-host combinations, concentrations, and morphologies for specific target analytes. Such computational approaches can significantly reduce trial-and-error in sensor development (Afshani et al., 2023; Bharadwaj et al., 2023; Chu et al., 2020).

8.2. *Multi-functional Sensors*

Future research will focus on integrating colorimetric sensing with electrochemical or optical transduction methods to develop multi-modal devices. This could enhance sensitivity, broaden detection ranges, and allow cross-validation of results in real time (Bharadwaj et al., 2023; Chu et al., 2020; Dhiman et al., 2023).

8.3. *Biocompatible Synthesis*

Green chemistry strategies—such as using plant extracts, agricultural waste, or polysaccharides as reducing/capping agents—offer eco-friendly and safer routes for synthesizing doped nanoparticles. These approaches reduce toxicity and improve compatibility for biomedical and environmental applications (Bharadwaj et al., 2023; Ferreiro et al., 2023; Khatkar et al., 2023).

8.4. *Wearable and Portable Platforms*

Embedding doped nanomaterials into flexible substrates like textiles, papers, and polymers enables low-cost, disposable, and portable sensors. Such wearable systems could find applications in personal health monitoring, environmental surveillance, and food quality control (Chen et al., 2021; Dhiman et al., 2023; Hastir et al., 2022).

9. CONCLUSION

The incorporation of transition and rare earth metal dopants into nanoparticles offers a versatile and effective strategy to engineer their optical, electronic, and structural properties for advanced colorimetric sensing applications. Dopant-induced modifications in band structure, defect density, and surface chemistry directly influence the sensitivity, selectivity, and operational stability of these systems. The type and concentration of dopants play a decisive role in modulating sensor performance, including detection limits, response times, and the extent of observable color change. Transition metal dopants such as Cu^{2+} and Fe^{3+} enhance visible-light absorption and charge transfer processes, while rare earth dopants like Eu^{3+} and Tb^{3+} introduce unique emission characteristics suitable for ratiometric sensing. This review highlights that rational selection of dopants, precise control over nanoparticle morphology, and the adoption of optimized synthesis methodologies are essential for realizing high-performance sensing platforms. Looking ahead, the integration of machine learning-assisted material design with sustainable, green synthesis approaches holds great promise in accelerating the development of wearable, portable, and real-time monitoring devices. Collectively, doped nanoparticle-based colorimetric sensors represent a significant step toward next-generation analytical technologies with broad applicability in environmental monitoring, biomedical diagnostics, and industrial safety.

10. REFERENCES

Afshani, J., Delgado, T., & Rosspeintner, A. (2023). Luminescence spectroscopy of Eu^{3+} in ternary aluminates. Journal of Luminescence, 263, 120043. https://doi.org/10.1016/j.jlumin.2023.120043

Anand, K. V., Karl Chinnu, M., Kumar, R. M., Mohan, R., & Jayavel, R. (2011). Controlled synthesis of Ce-doped ZnS nanoparticles. International Journal of Nanoscience, 10(03), 487–493. https://doi.org/10.1142/S0219581X11008516

Bharadwaj, M., Singh, S. P., Rai, S. B., & Kumar, D. (2023). Color tunable upconversion in Pr-Yb co-doped titania silicate glass ceramic. Optical Materials, 146, 114492. https://doi.org/10.1016/j.optmat.2023.114492

Cardillo, D., Konstantinov, K., & Devers, T. (2013). The effect of cerium doping on the UV filtration and structural properties of α-hematite nanoparticles. Materials Research Bulletin, 48(11), 4521–4528. https://doi.org/10.1016/j.materresbull.2013.07.042

Chen, Z. Y., Zhang, Y., Zhang, W. J., Dong, G. P., Zhou, S. F., & Qiu, J. R. (2021). Programmable broadband responsive lanthanide-doped nanoarchitecture for information encryption. Advanced Optical Materials, 10(1), 2101843. https://doi.org/10.1002/adom.202101843

Chu, H., Zhang, Y., Wang, J., & Wang, L. (2020). Double emission rationetric fluorescent sensors of rare-earth-doped ZnS quantum dots for Hg^{2+} detection. ACS Omega, 5(16), 9558–9565. https://doi.org/10.1021/acsomega.0c00813

Derom, S., Berthelot, A., Pillonnet, A., & Benamara, O. (2013). Metal enhanced fluorescence in rare earth doped plasmonic core-shell nanoparticles. arXiv. https://arxiv.org/abs/1305.2745

Dey, P. A., & Choudhury, S. (2019). Structural, optical and gas sensing properties of Fe-doped SnO_2 nanoparticles. Ceramics International, 45(10), 12625–12633. https://doi.org/10.1016/j.ceramint.2019.03.055

Dhiman, P., Rana, G., Kumar, A., & Dawi, E. A. (2023). Rare earth doped ZnO nanoparticles as spintronics and photocatalyst for degradation of pollutants. Molecules, 28(6), 2838. https://doi.org/10.3390/molecules28062838

Ferreiro, A., Galdámez, A., Barahona, T., Peña, O., & Marco, J. F. (2023). Effect of lithium codoping on the structural, optical and magnetic properties of Nd-doped ZnO. Ceramics International, 49(19), 33513–33524. https://doi.org/10.1016/j.ceramint.2023.03.098

Haase, M., & Schäfer, H. (2019). Upconverting nanoparticles. Angewandte Chemie International Edition, 50(26), 5808–5829. https://doi.org/10.1002/anie.201005159

Hastir, A. F., Kumar, R., Singh, R. C., & Sharma, J. (2022). The effect of rare earths on the response of photo UV activate ZnO gas sensors. Sensors, 22(21), 8150. https://doi.org/10.3390/s22218150

Hou, T., Mao, J., Zhu, X., & Tu, M. (2006). STM/STS investigations of Ce-doped TiO_2 nanoparticles. Rare Metals, 25(4), 331–336. https://doi.org/10.1016/S1001-0521(08)60097-5

Kabir, M. H., Ali, M. M., Hossain, M. S., Hossain, K. S., & Rahman, M. M. (2023). Enhancement of photocatalytic performance of V_2O_5 by rare-earth ions doping (Ho^{3+}/Yb^{3+}). Materials Chemistry and Physics, 305, 127941. https://doi.org/10.1016/j.matchemphys.2023.127941

Khan, S. S. (2015). Visible light photocatalytic enhancement of CdO-ZnO nanohybrids. Journal of Photochemistry and Photobiology B: Biology, 142, 1–7. https://doi.org/10.1016/j.jphotobiol.2014.11.001

Khatkar, A., Kumar, R., & Lata, S. (2023). Cool white emission in $Ba_2LaV_3O_{11}$:Dy^{3+} nanophosphors for WLEDs. Solid State Communications, 375, 115356. https://doi.org/10.1016/j.ssc.2023.115356

Krajnik, B., Golacki, L. W., Mackowski, S., & Caterina, M. (2021). Quantitative comparison of luminescence probes for biomedical applications. Methods and Applications in Fluorescence, 9(4), 045001. https://doi.org/10.1088/2050-6120/ac1a9e

Lee, J. S., Noh, T. H., & Kim, I. G. (2013). Doping strategies for nanomaterial-based magnetism. Journal of Materials Chemistry C, 1(5), 4925–4932. https://doi.org/10.1039/c3tc00174a

Loo, J. F. C., Chien, Y. H., Yin, F., Kong, S. K., Ho, H. P., & Yong, K. T. (2019). Upconversion and downconversion nanoparticles for biophotonics and nanomedicine. Nanoscale, 11(40), 18504–18524. https://doi.org/10.1039/c9nr04487a

Muthuvel, A., Jothibas, M., Manoharan, C., & Jayakumar, S. J. (2020). Synthesis and improvement of photocatalytic and optical properties of Ce doped CdO and ZnO nanoparticles. Research on Chemical Intermediates, 46(5), 2705–2729. https://doi.org/10.1007/s11164-020-04111-0

Ong, C. B., Ng, L. Y., & Mohammad, A. W. (2022). A review of rare-earth (RE) doped ZnO for optoelectronic applications. Nanoscale Advances, 4(9), 1868–1885. https://doi.org/10.1039/d1na00879c

Patil, S. B., & Devan, R. S. (2020). HRTEM analysis of Fe-doped SnO_2 nanoparticles for optoelectronic applications. Applied Surface Science, 507, 145123. https://doi.org/10.1016/j.apsusc.2019.145123

Shanmugam, A., & Murugasen, P. (2018). Morphological and optical modifications of Zn-doped CuO nanoparticles synthesized by hydrothermal method. Materials Research Express, 5(4), 045013. https://doi.org/10.1088/2053-1591/aab9f1

Shkir, M., AlFaify, S., Arora, M., Algarni, H., & Singh, B. P. (2020). Investigation on structural, morphological, linear and third order nonlinear optical properties of sol-gel derived Sm-doped CdS thin films for photodetector applications. Sensors and Actuators A: Physical, 306, 111952. https://doi.org/10.1016/j.sna.2020.111952

Singh, A., Sambyal, S., Singh, V., Kaur, B., & Sharma, A. (2023). Nanocomposite metal oxide for optoelectronic applications. In S. Kumar & P. Singh (Eds.), Advanced nanomaterials for optoelectronic applications (pp. 45–67). Elsevier.

Srisuvetha, V. T., Rayar, S. L., & Shanthi, G. (2020). Role of Ce dopant in MgO nanoparticles on the structural, optical, dielectric, and magnetic properties. Journal of Materials Science: Materials in Electronics, 31(4), 2799–2808. https://doi.org/10.1007/s10854-019-02819-3

Tian, S. L., Li, Y., Sun, S. K., & Xu, X. H. (2022). Color tunable persistent luminescence $LiTaO_3$:Pr^{3+} for dynamic anti-counterfeiting. Journal of Alloys and Compounds, 899, 163325. https://doi.org/10.1016/j.jallcom.2021.163325

Tripathi, R. M., Shrivastav, A., & Shrivastav, B. R. (2017). Structural and optical studies of Cu-doped ZnO nanoparticles synthesized by sol-gel method. Journal of Materials Science: Materials in Electronics, 28(16), 12363–12371. https://doi.org/10.1007/s10854-017-7054-8

Venkatesu, P. (2013, July). Doping effect of Mn on properties of CdS nanoparticles. International Conference on Nanomaterials, Barcelona, Spain.

Wang, J., Ma, C., Chen, M., Kim, H. Y., Li, Y., & Liu, F. (2019). Advanced dynamic photoluminescent material for anticounterfeiting. ACS Applied Materials & Interfaces, 11(38), 35871–35878. https://doi.org/10.1021/acsami.9b09775

Wikipedia contributors. (n.d.). Upconverting nanoparticles. In Wikipedia, The Free Encyclopedia. Retrieved November 28, 2023, from https://en.wikipedia.org/wiki/Upconverting_nanoparticles

Xu, L. N., Li, L. L., Wang, Y., Tu, D., Sun, Y. J., & Chen, X. Y. (2021). Multicolour luminescence of $NaYF_4$:Yb^{3+}/Ho^{3+}/Ce^{3+} microcrystals under 940 nm excitation. Journal of Rare Earths, 40(3), 406–414. https://doi.org/10.1016/j.jre.2021.04.013

Zelaya-Angel, O., Alvarado-Gil, J. J., Lozada-Morales, R., Vargas, H., da Silva, A. F., & de Oliveira, I. N. (2012). Erbium doping enhances photoluminescence in CdS thin films. Journal of Materials Science, 47(1), 479–485. https://doi.org/10.1007/s10853-011-5817-9

Zhang, J. C., Zhao, X. B., Wang, Y. X., & Xia, Z. G. (2018). Thermo-mechano-opto responsive bistable luminescence in lanthanide phosphors. Advanced Materials, 30(50), 1804644. https://doi.org/10.1002/adma.201804644